Urban-rural shifts in elemental composition in leaves and topsoil of street trees in a subtropical city of China

Urban Forestry and Urban Greening

He, Tao; Du, Enzai; Yang, Xueyi; Guo, Yuying; Xia, Nan et al

https://doi.org/10.1016/j.ufug.2025.128677

Urban Forestry & Urban Greening 104 (2025) 128677

Contents lists available at ScienceDirect

Urban Forestry & Urban Greening

journal homepage: www.elsevier.com/locate/ufug

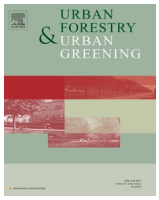

Urban-rural shifts in elemental composition in leaves and topsoil of street trees in a subtropical city of China

Tao He [a,b], Enzai Du [a,b,*], Xueyi Yang [a,b], Yuying Guo [a,b], Nan Xia [a,b], Wim de Vries [c]

[a] State Key Laboratory of Earth Surface Processes and Resource Ecology, Faculty of Geographical Science, Beijing Normal University, Beijing 100875, China
[b] School of Natural Resources, Faculty of Geographical Science, Beijing Normal University, Beijing 100875, China
[c] Wageningen University and Research, Earth Systems and Global Change Group, PO Box 47, Wageningen 6700 AA, the Netherlands

ARTICLE INFO

Keywords:
Macronutrient
Trace element
Urban street
Principal component analysis
Spatial pattern
Urban hotspot

ABSTRACT

Street trees provide essential ecosystem services and are subject to large inputs of anthropogenic-sourced elements and frequent management operations. However, a systematic understanding of the elemental composition in street tree leaves and topsoil is still lacking. Based on a field survey across urban-rural gradients in a subtropical city (Chengdu) of China, we explored the spatial patterns of ten elements (i.e., nitrogen (N), phosphorus (P), potassium (K), calcium (Ca), magnesium (Mg), aluminum (Al), iron (Fe), zinc (Zn), copper (Cu) and chromium (Cr)) in street tree leaves and in topsoil (0–10 cm) as well as their key drivers. Our results indicate that leaf N, P, K, and Al contents as well as topsoil N, P, and Al contents showed a significant increase toward the central urban area. In contrast, no significant spatial trends were found for other elements across the urban-rural gradients. The first principal component of leaf elemental composition (mainly explained by N, K, Mg, Fe, Cu, and Al contents) and the second principal component of topsoil elemental composition (mainly explained by P, K, Mg, Fe, and Al contents) both increased significantly toward the central urban area. Unexpectedly, leaf and topsoil elemental composition showed no significant correlations with each other. Our findings demonstrate distinctive spatial patterns of the elemental composition of leaf and topsoil for street trees across urban-rural gradients and highlight a decoupling between leaf and topsoil element composition in the street tree systems. These results improve our understanding of how urbanization reshapes the pattern of biogeochemical cycling and provide a baseline for better nutrient management in the street tree systems.

1. Introduction

Biogeochemical cycles in urban forests are intensively altered by anthropogenic activities (Lorenz and Lal, 2009; Kaushal et al., 2014; Shurpali, 2023). Street trees, growing in tree pits along roads, are an important component of urban forests (Mullaney et al., 2015). Compared to natural forests or trees growing in urban parks, street trees are generally subjected to more air pollutants, especially from transportation-related sources (Dan-Badjo et al., 2008; Bettez et al., 2013). Road air quality often is the worst within urban areas due to high vehicular emissions of pollutants (Bettez et al., 2013). Previous studies mainly focused on the ecosystem services provided by street trees, such as filtering air pollutants, storing carbon, providing shade, reducing noise, and ameliorating the urban heat-island effect (Janhäll, 2015; Mullaney et al., 2015; McPherson et al., 2016; Willis and Petrokofsky, 2017; Liu et al., 2023). However, the urban-rural shifts in multiple elements in street trees along with changes in the inputs of the air pollutants remain largely unknown. Moreover, street trees generally grow in isolated tree pits where element cycling is blocked by management operations (e.g., litter removal) and impervious surrounding surfaces (Fig. 1a). These characteristics of element cycling in street tree systems (including street trees and the underlying soil) likely shape distinctive elemental composition of street trees and underlying topsoil which remain poorly understood.

Street tree systems receive chronic inputs of various anthropogenic-sourced elements (Fig. 1a). Specifically, traffic-sourced elements are mainly from gasoline combustion process, gasoline additives, catalytic converters (e.g., NO_x reduction agent, and tricresyl phosphate), metal

* Corresponding author at: State Key Laboratory of Earth Surface Processes and Resource Ecology, Faculty of Geographical Science, Beijing Normal University, Beijing 100875, China.
E-mail address: enzaidu@bnu.edu.cn (E. Du).

https://doi.org/10.1016/j.ufug.2025.128677
Received 20 October 2024; Received in revised form 10 January 2025; Accepted 13 January 2025
Available online 15 January 2025

containers, pipes and devices used in gasoline production, storage and transportation, as well as the wear of tyre and engine components and lubricating oil (Miller et al., 2007; Ministry of Ecology and Environment of the People's Republic of China, 2013; Wild et al., 2017; Wang et al., 2017a; Coufalík et al., 2019; Indris et al., 2020). Generally, non-heavy metal elements (e.g., Ca, Mg, Fe, and Al) are found to account for ~80 % of the metal elements in the diesel fuel and the remaining ~20 % are heavy metal elements (e.g., Cr, Zn, and Cu) (Wang et al., 2003). Additionally, street tree pits receive element inputs from other occasional anthropogenic sources, such as occasional fertilization, dumping of household waste or building materials, although they are hard to be quantified (Nielsen., 2019; Kaushal et al., 2020; Xiong et al., 2020; Fig. 1a). Overall, the abovementioned human activities are generally more intensive in urban areas, likely shaping a decrease in the magnitude of their impacts on the elemental composition of street tree systems across the urban-rural gradients.

The elemental composition of topsoil in street tree pits is strongly reshaped by human activities compared to that in the natural forests (Kaye et al., 2006; Lorenz and Lal, 2009; Dynarski et al., 2023). For instance, vehicular emission, mostly deposited within a distance of 20 m, is an important source for the topsoil element inputs (Trombulak and Frissell, 2000; Dan-Badjo et al., 2008; De Silva et al., 2016; Fig. 1a). The bulk deposition of K, Ca, and Mg in large cities is high and shows a significant decrease with the distance to the city (Du et al., 2018). Additionally, non-exhaust emissions (e.g., particles from brake pads, tires, belts, road paint) as well as some occasional anthropogenic sources (e.g., pet dogs, occasional fertilization) are also important sources for topsoil elements (Nielsen, 2019; Jeong et al., 2022). Moreover, compared to natural ecosystems, nutrient inputs from litterfall and consequent decomposition are largely blocked in the street tree systems due to impervious surface and litter removal, resulting in a significant element loss over time (Bradford et al., 2016; Chen et al., 2018; Fig. 1a). In view of urban-rural changes in anthropogenic-sourced inputs, topsoil elemental contents in street tree pits likely show an increase toward the urban core (Fig. 1b).

Street trees may adjust their leaf elemental composition in response to changes in external element inputs and soil nutrient availability (Kaye et al., 2006; Cobley and Pataki, 2019). Street trees take up nutrients from soils through a combination of pathways, including direct root absorption and associations with mycorrhizal fungi (Day et al., 2010; Anbarasan and Ramesh, 2021). In addition to root nutrient uptake from soils (Olowoyo et al., 2010; Przybysz et al., 2014; Fig. 1a), street trees can also assimilate vehicular-emitted elements through leaf stomata and cuticles (Oliva and Espinosa, 2007; Fig. 1a). The magnitudes of nutrient assimilation by these two pathways depend on the soil nutrient availability in tree pits and on the air concentrations of vehicular-emitted gases (e.g., NOx) or the solubility of deposited particles, respectively (Sanchez-Lopez et al., 2015; Song et al., 2015; Rai, 2016). Moreover, the capacity of leaf nutrient assimilation varies among tree species with different nutrient demands (Xu et al., 2018). In view of a potential decrease in the nutrient inputs from human activities across urban-rural gradients, the leaf elements of street trees may decrease from central urban area to rural area (Du et al., 2022a; Fig. 1c).

The elemental composition of street tree leaf and topsoil may thus show a significant change across urban-rural gradients, while such a hypothesized spatial pattern remains unexplored. The urbanization of Chengdu, a subtropical large city in Sichuan province of China, is characterized by periodic expansion: initially concentrated within the first ring road before 1970s, and concentrically expanded to the second ring road during 1980s–1990s and then concentrically expanded to the third ring road after 1990s (Fig. 2c; Wang et al., 2017b). By systemically sampling street tree leaves and topsoil (0–10 cm) across urban-rural gradients in Chengdu, we explored the spatial patterns and main drivers of ten element contents (N, P, K, Ca, Mg, Al, Fe, Zn, Cu, and Cr) in leaf and topsoil samples. Specifically, we tested the following hypotheses: (i) leaf and topsoil contents of anthropogenic derived elements in street tree systems both increase significantly towards the urban core due to more intensive inputs via human activities (urban hotspot

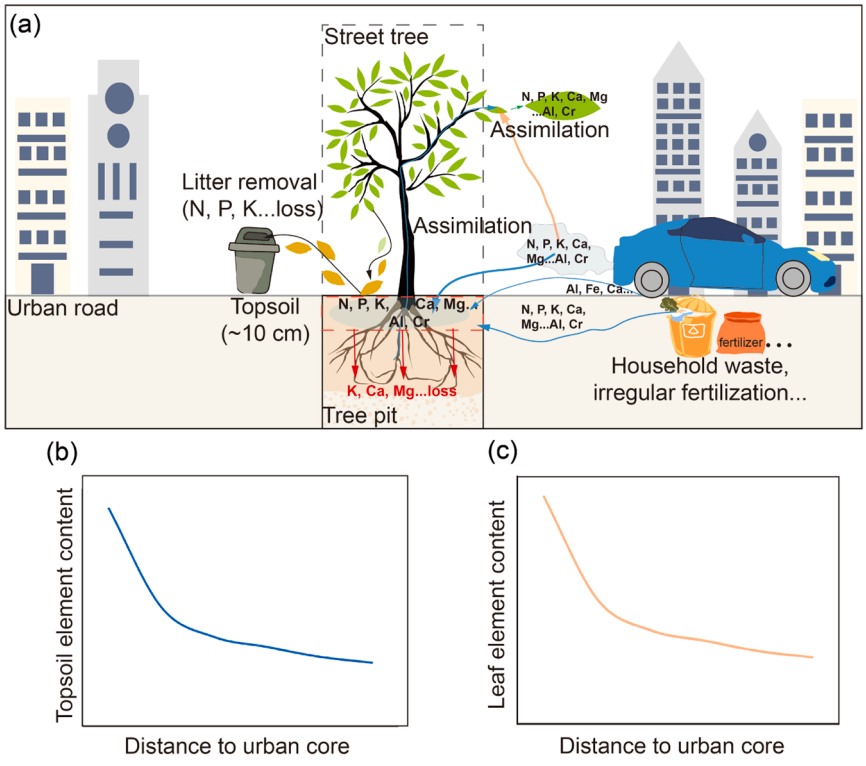

Fig. 1. Conceptual diagram of element cycling in the street tree system (a), and the hypothesized changes in traffic-sourced element contents of tree pit topsoil (b) and street tree leaves (c) across the urban-rural gradients.

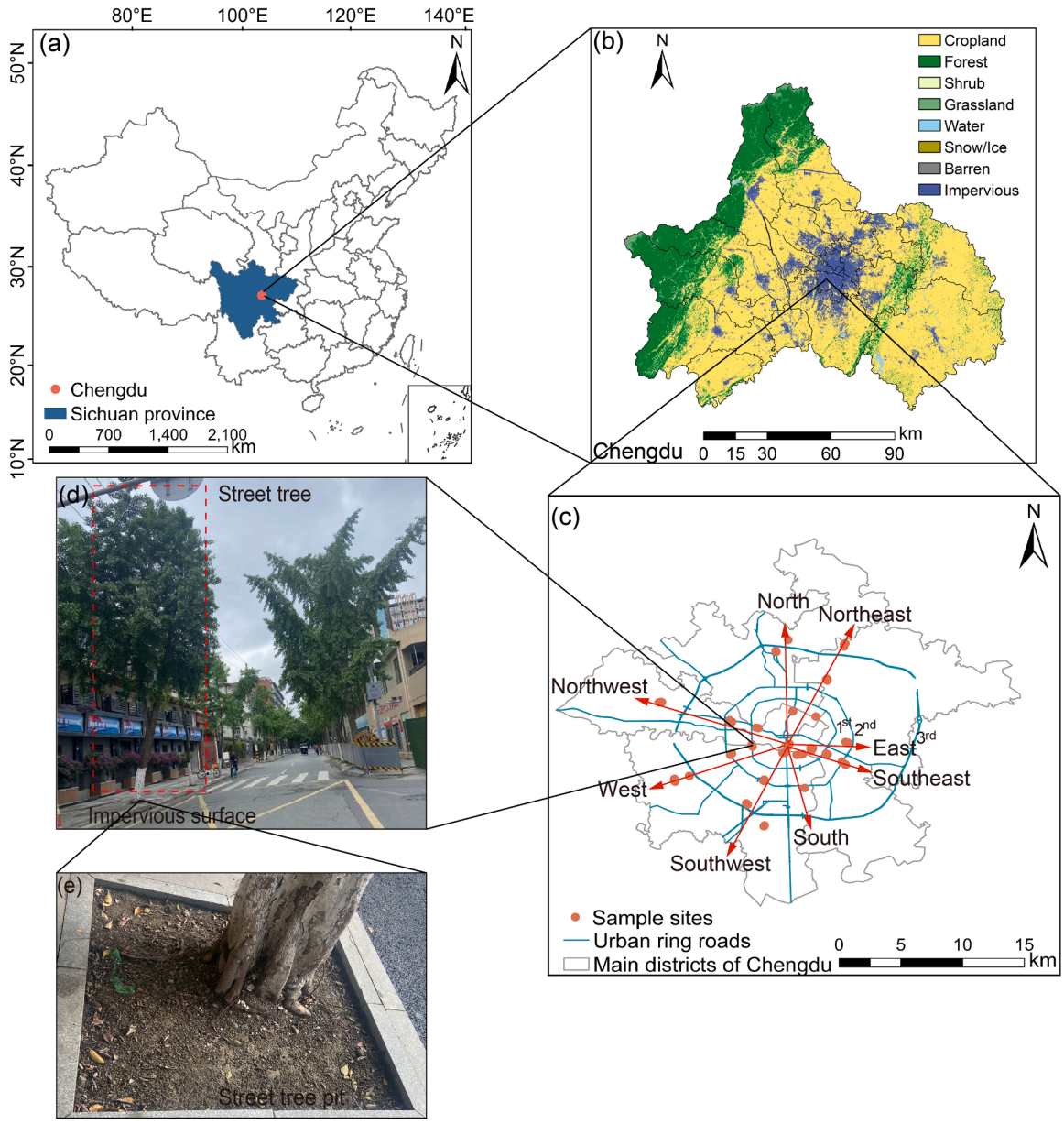

Fig. 2. The study area (Chengdu, China) (a-b), the locations of the sampling sites (25 sites across seven directions) (c), and photos of an example street tree (d) and street tree pit (e). Land use information (2022) was derived from Yang and Huang (2023).

hypothesis); (ii) leaf and topsoil elemental composition are coupled due to the urban-rural gradients of anthropogenic element inputs into the street tree systems and the elemental uptake of street trees from topsoil (plant-soil coupling hypothesis).

2. Materials and methods

2.1. Study area

Chengdu city, located in Chengdu Plain in the southwest of China (Fig. 2a, b), is one of the largest cities in China. Chengdu is featured with a subtropical humid monsoon climate with mean annual temperature (MAT) of 17.3 °C and annual precipitation (AP) of 984 mm, respectively (Chengdu Municipal Bureau of Statistics, 2023). The urban area in Chengdu has expanded continuously in recent decades and the urban resident population has grown to over 16 million with the land area of over 14,000 km^2 (Chengdu Municipal Bureau of Statistics, 2023). Chengdu's central areas (i.e., residential and commercial areas) with high population density are primarily concentered within the first ring road, and its rural areas (i.e., industrial and ecological areas) are mainly located beyond the third ring road (Fig. 2c; Wang et al., 2017b). The road network has a total length of more than 9400 km and the density of road network generally decreases from central urban areas to peri-urban and rural areas. Street trees in Chengdu are dominated by weeping fig tree (*Ficus concinna* Miq.), ginkgo tree (*Ginkgo biloba* L), and white fig tree (*Ficus virens* Aiton) (Zong et al., 2020). Among these three species, ginkgo tree, and white fig tree are two native species, while weeping fig tree is an introduced species (Zong et al., 2020; Table S1).

2.2. Field sampling

Field sampling was conducted from 2 August to 12 August 2022 following a stratified random sampling approach (Tang et al., 2016). The stratified random sampling approach is a high-efficiency method of sample selection that first divides into smaller strata based on shared characteristics of the samples and then randomly selects among each

stratum to form the final sample (Nickolas, 2021). Here, the sampling roads (i.e., strata) were selected based on the locations of ring roads and street tree species, and then street trees were randomly selected on each sampling road (i.e., stratum)..

Specifically, we selected one sampling site at the urban core (i.e., Tianfu Square) and 24 sampling sites along eight directions from the central urban area to the rural areas (i.e., north, northeast, east, southeast, south, southwest, west, and northwest) (Fig. 2c, Table S1). At each sampling site, three street trees were randomly selected (see a photo of an example street tree in Fig. 2d and e) and mature leaves were sampled from street tree crowns using a high branch scissor. Topsoil samples were randomly collected from street tree pits at a depth of 0–10 cm using an auger (diameter = 5 cm) (Fig. 2e). Our sampling focused on topsoil because (i) anthropogenic-sourced element inputs mostly accumulate in topsoil (De Vries et al., 1994; Serbula et al., 2012; Fantozzi et al., 2013; Cetin et al., 2022), (ii) a major proportion of the nutrient uptake takes place in topsoil layer (Jobbagy and Jackson, 2001), and (iii) it is difficult to collect samples of deep soils in street tree pits. Diameter at breast height (DBH), life form (evergreen or deciduous), and the street tree species were recorded.

2.3. Laboratory measurement

Leaf samples were carefully rinsed using deionized water to remove dust-borne particles and then dried at 65 °C for 48 hours (Xia et al., 2023). Dried leaf samples were ground using a mill (NM200, Retsch, Germany), and passed through a 0.149 mm mesh (Xia et al. 2023). Topsoil samples were air-dried at room temperature and sieved through a 2-mm mesh to remove coarse organic debris and small gravels (Xia et al., 2022; Guo et al., 2024). Small visible roots were picked out manually (Guo et al., 2024). For each topsoil sample, a subsample was used to measure topsoil pH, and the remaining part was milled and sieved through a 0.149 mm mesh for the measurement of element contents. Topsoil pH was measured using a pH meter (soil:water ratio 1:2.5) (PB-10, Sartorius, Germany) (Soil Survey Staff, 2014). The C and N contents in leaf and topsoil were measured using an isotope ratio mass spectrometer (Thermo Delta V, Thermo Fisher Scientific Inc, Newton Drive, Carlsbad, USA). Table S2

Leaf and topsoil samples were completely digested with nitric, hydrofluoric, and perchloric acids with a ratio of 3:2:1 in a microwave digestion system (MARS 6 Xpress, CEM, Mattews, North Carolina, USA) (Douvris et al., 2023). The contents of P, K, Ca, Mg, Al, Fe, Zn, Cu, and Cr in the leaf and topsoil samples were then measured using an inductively coupled plasma optical emission spectrometer (ICP-OES, Optima 8000, PerkinElmer, USA) (Douvris et al., 2023). https://jjg.spc.org.cn Before our formal sample test, we used a mixed multi-element standard solution (GBW€081531) to ensure the accuracy and precision of measurement. The correlation coefficient between mixed multi-element standard solution concentrations and spectral intensity exceeded 0.999. We made calibration every two hours during our measurement. Moreover, the relative standard deviation of corrected spectral intensities shows the fluctuation of spectral intensity, reflecting the stability of emission spectrometer (i.e., precision of instrument). The relative standard deviation of concentration in calibration units shows the fluctuation of the calculation of elemental concentration using calibration standard curve, reflecting the accuracy and precision of elemental concentration measurements. In this study, the mean relative standard deviation of corrected spectral intensities and concentration in calibration units for the sample element analysis (i.e., P, K, Ca, Mg, Al, Fe, Zn, Cu, and Cr) ranged from 1.7 % to 2.8 %, and 1.7 % to 6.0 %, respectively, implying a good accuracy and precision of measurements (Table S2).

2.4. Data on potential drivers

To identity the key drivers of the spatially varying elemental composition in street tree leaves and topsoil, we collected data on anthropogenic (road network density, RD; road width, RW; road age, RA;), climatic (MAT and AP), edaphic (topsoil pH and topsoil C: N), and tree specific variables (DBH and life form) (Table S1). Specifically, road network density (km km^{-2}) was calculated as the total length of the main roads (i.e., primary and secondary roads) in an area with a radius of 1 km from each sampling site (Cobley and Pataki, 2019; Du et al., 2022b). The length of the main road in Chengdu was derived from the National Catalogue Service for Geographic Information (https://www.webmap.cn/). Road width was derived from Baidu Map (https://map.baidu.com/). Road age was derived from Chengdu Transport Bureau (http://jtys.chengdu.gov.cn/). Data on MAT and AP of the sampling year were derived from the National Tibetan Plateau Data Center with a spatial resolution of 1 km (http://data.tpdc.ac.cn/). Information on the DBH, life form, topsoil pH, and topsoil C:N were measured and recorded in this study (See Sections 2.2 and 2.3). The distance to the urban core was defined as the distance from each sampling site to Tianfu Square and was derived using Arc GIS 10.7 (ESRI, Redlands, CA, USA).

2.5. Statistical analysis

Data on topsoil and leaf element contents were $\log_{10}$-transformed to a normal distribution for further analysis. The Lilliefors test was conducted to test the normality of $\log_{10}$-transformed leaf and topsoil element contents, as well as the principal components of leaf and topsoil elements (Lilliefors., 1967). Lilliefors test is a nonparametric statistical approach to test the normality of data distribution particularly powerful for data with sample sizes ($n < 30$) (Lilliefors, 1967). We conducted regression analysis to explore the spatial trends in element contents in street tree leaves and topsoil (i.e., N, P, K, Ca, Mg, Al, Fe, Zn, Cu, and Cr) with the distance to the urban core. To analyze the characteristics of leaf and topsoil elemental composition, principal component analysis (PCA) was conducted using '*stats*' package (Venables and Ripley, 2002). To do so, original data of leaf and topsoil element contents were first $\log_{10}$--transformed and normalized. Regression analysis was then conducted to demonstrate the changes of the first two principal components (PC1 and PC2) of elemental composition with the distance to the urban core. Finally, correlation analysis was conducted to test the correlations between leaf and topsoil elemental compositions.

To identify key drivers explaining the spatial patterns of leaf and topsoil element contents, redundancy analysis (RDA) and hierarchical partitioning analysis were conducted using the '*vegan*' and '*rdacca.hp*' packages (Lai et al., 2022). Redundancy analysis was used to show general relationships between all the potential drivers and leaf and topsoil element contents. The variance inflation factor (VIF) was calculated and used to distinguish the multicollinearity (VIF < 3 indicates weak collinearity) of the potential drivers (Zuur et al., 2010). Then, hierarchical partitioning analysis was used to estimate the independent variance explained by each driver (Table S2 and Table S3; Lai et al., 2022). Moreover, redundancy analsysis and hierarchical partitioning analysis were also used to explore the key drivers to shape the spatial patterns of leaf and topsoil PC1 and PC2. All statistical analyses were conducted using R software (version 4.0.0, R Development Core Team, http://www.r–project.org/) with a significance level at $p < 0.05$.

3. Results

3.1. Urban-rural gradients and drivers of topsoil element contents

Log_{10}-transformed data on topsoil elements generally followed a normal distribution (Lilliefors test: $p > 0.05$; Table S3). The $\log_{10}$-transformed values of N, P, and Al contents in tree pit topsoil exhibited a decrease with a larger distance to the urban core (N: $r^2 = 0.16$, $p = 0.049$; P: $r^2 = 0.52$, $p < 0.0001$; Al: $r^2 = 0.16$, $p = 0.047$; Fig. 3a, b, and f). However, other elements (i.e., K, Ca, Mg, Fe, Zn Cu, and Cr) showed no significant trends across the urban-rural gradients (K: $p = 0.533$; Ca: $p = 0.782$; Mg: $p = 0.147$; Fe: $p = 0.719$; Zn: $p = 0.278$;

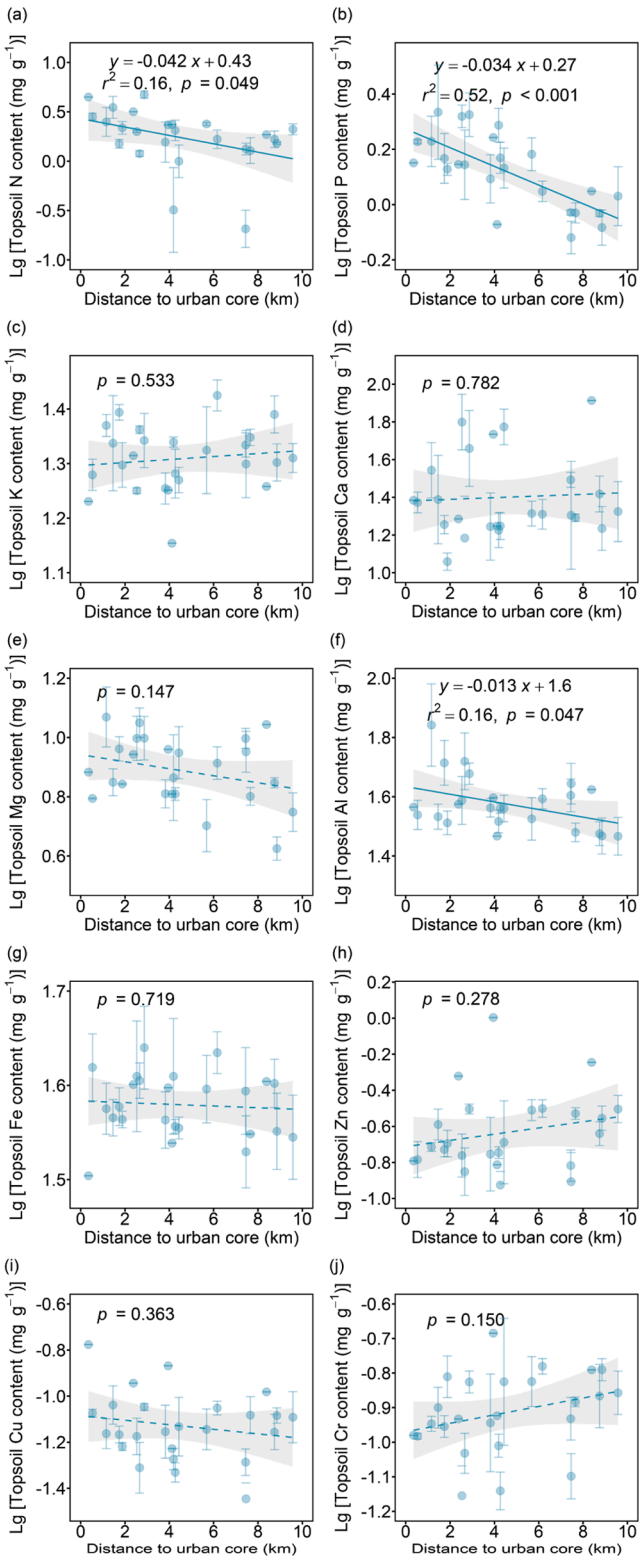

Fig. 3. Changes in topsoil contents(log_{10}-transformed) of N (a), P (b), K (c), Ca (d), Mg (e), Al (f), Fe (g), Zn (h), Cu (i) and Cr (j) with the distance to the urban core. The error bar indicates the standard error of repeated samples. The shaded areas indicate the 95 % confidence intervals of the curve fit.

Cu: $p = 0.363$; Cr: $p = 0.150$; Fig. 3c–e and Fig. 3g–j). The hierarchical partitioning analysis of variance showed that the seven drivers (road age, road width, road density, AP, MAT, topsoil pH, and diameter at breast height) jointly explained 32 %, 40 %, and 39 % of the spatial variation in topsoil N, P, and Al contents, respectively (Fig. S1). Specifically, road age accounted for 72 %, 54 %, and 41 % of the total variance explained by all the seven drivers for topsoil N, P, and Al, respectively (Fig. S1). Higher topsoil contents of N, P, and Al were found for tree pits along older roads (N: variance explained = 24 %, $p < 0.01$; P: variance explained = 22 %, $p < 0.01$; Al: variance explained = 16 %, $p < 0.05$; Fig. S1d–f, Table S4).

3.2. Urban-rural gradients and drivers of leaf element contents

Log_{10}-transformed data on leaf elements generally followed a normal distribution (Lilliefors test: $p > 0.05$; Table S3). The log_{10}-transformed values of N, P, K, and Al contents in street tree leaves showed significant trends across the urban-rural gradients ($p < 0.05$) (Fig. 4). Specifically, leaf N content exhibited a nonlinear pattern across urban-rural gradients ($r^2 = 0.32, p = 0.014$), and decreased significantly with a distance larger than 4 km to the urban core (Fig. 4a). The log_{10}-transformed values of P, K, Ca, and Al contents in street tree leaves showed a significant decrease with increasing distance to the urban core (P: $r^2 = 0.30$, $p = 0.004$; K: $r^2 = 0.35$, $p = 0.002$, Al: $r^2 = 0.20$, $p = 0.026$; Fig. 4b, c, and f). In contrast, the contents of Ca, Mg, Fe, Zn, Cu, and Cr in leaf samples showed no significant variations across urban-rural gradients (Ca: $p = 0.140$; Mg: $p = 0.976$; Fe: $p = 0.108$, Zn: $p = 0.464$; Cu: $p = 0.107$; Cr: $p = 0.567$; Fig. 4d, e, g–j). Redundancy analysis indicated that road age, MAT, and AP were three key predictors of the spatial trends of leaf element contents (Fig. S2a). Hierarchical partitioning analysis of variance showed that the nine drivers (road age, road width, road density, AP, MAT, topsoil pH, topsoil C: N, life form, and diameter at breast height) jointly explained 69 %, 62 %, 54 %, and 42 % of the spatial variations in leaf N, P, K, and Al contents, respectively (Fig. S2b–S2c). Specifically, leaf P and K contents were positively correlated with MAT and AP, respectively (P: variance explained = 14 %, $p < 0.05$; K: variance explained = 20 %, $p < 0.05$; Fig. S2e & S2f, Table S5). Leaf N and Al contents were higher for street trees of the older roads (N: variance explained = 14 %, $p = 0.14$; Al: variance explained = 11 %, $p = 0.097$; Fig. S2d & S2g, Table S5). Moreover, the contents of leaf N and P in the deciduous leaves showed a significant higher value than these in evergreen leaves (N: variance explained = 12 %, $p < 0.05$; P: variance explained = 14 %, $p < 0.001$; Fig. S3, Table S5).

3.3. Urban-rural shifts and drivers of leaf and topsoil elemental composition

Principal component analysis indicated that the first two principal components explained 51 % and 58 % of the total variance in the topsoil and leaf elemental composition, respectively (Fig. 5a and b; Table S6). Specifically, topsoil and leaf PC1 and PC2 both followed a normal distribution (Lilliefors test: $p > 0.05$; Table S3). PC1 and PC2 explained 29 % and 22 % of the total variance of the topsoil elemental composition, respectively (Fig. 5a). N, Ca, Zn, Cu, and Cr showed higher loading values on PC1, and the other five elements had higher loading values on PC2 (Table S6). Topsoil PC2 increased significantly towards the urban core ($p = 0.025$), while topsoil PC1 showed no significant variation across the urban-rural gradients ($p = 0.679$) (Fig. 5c and d). The hierarchical partitioning analysis of variance showed that only 27 % of the spatial pattern of topsoil PC2 was explained by the seven predictors (road age, road width, road density, AP, MAT, topsoil pH, and diameter at breast height) (Fig. 6b). Meanwhile, correlation analysis indicated that topsoil PC2 increased significantly with higher MAT (variance explained = 10 %; $p < 0.05$; Fig. 6c).

The first principal component (PC1) explained 37 % of the total variation of the leaf elemental composition with higher loadings of leaf N, K, Mg, Fe, Cu, and Al contents (Fig. 5b; Table S6). The second principal component (PC2) explained 21 % of the total variation of the leaf elemental composition, and leaf P, Ca, Zn, and Cr contents had a higher loading on it (Fig. 5b; Table S6). Leaf PC1 showed a significant increase

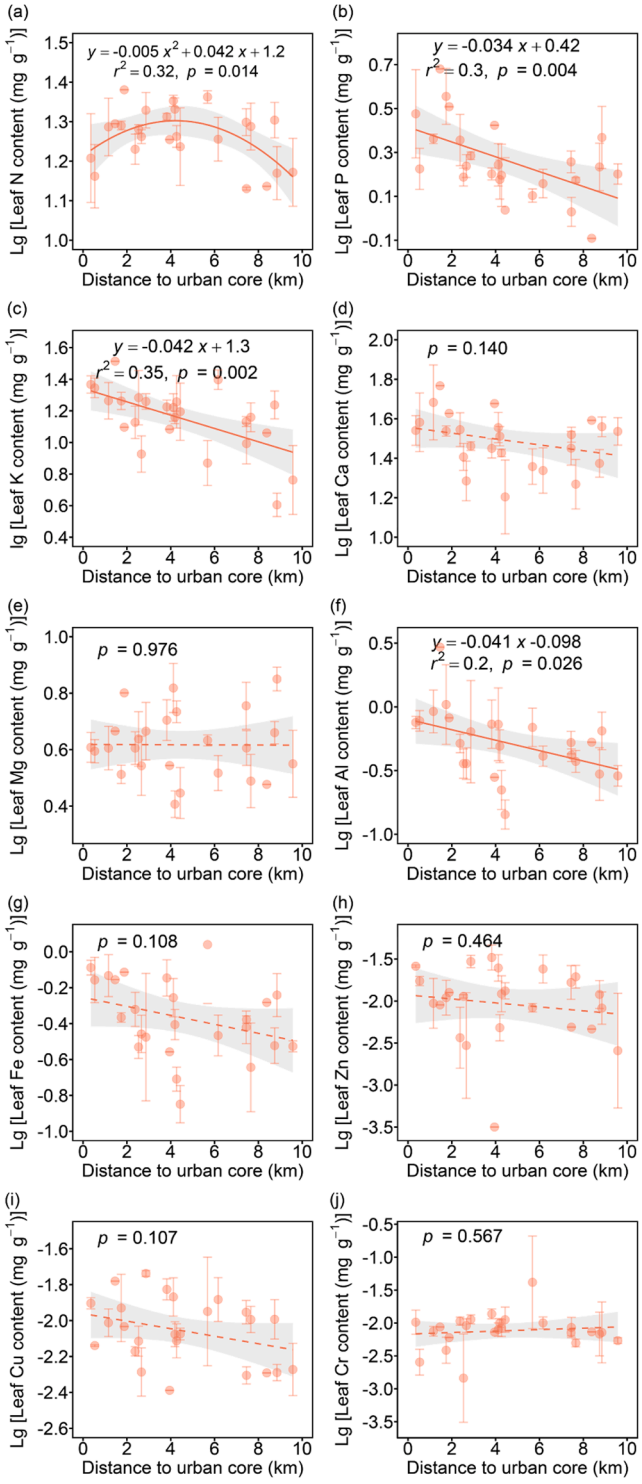

Fig. 4. Changes in leaf contents(log_{10}-transformed) of N (a), P (b), K (c), Ca (d), Mg (e), Al (f), Fe (g), Zn (h), Cu (i) and Cr (j) with the distance to the urban core. The error bar indicates the standard error of repeated samples. The shaded areas indicate the 95 % confidence intervals of the curve fit.

toward the urban core ($p = 0.029$; Fig. 5e), while no significant spatial variation was found for leaf PC2 across urban-rural gradients ($p = 0.373$; Fig. 5f). The hierarchical partitioning analysis of variance showed that nine drivers (road age, road width, road density, AP, MAT, topsoil pH, topsoil C: N, life form, and diameter at breast height) explained 61 % of the spatial pattern of leaf PC1 (Fig. 6b). Specifically, road age and life form were two most important drivers, jointly

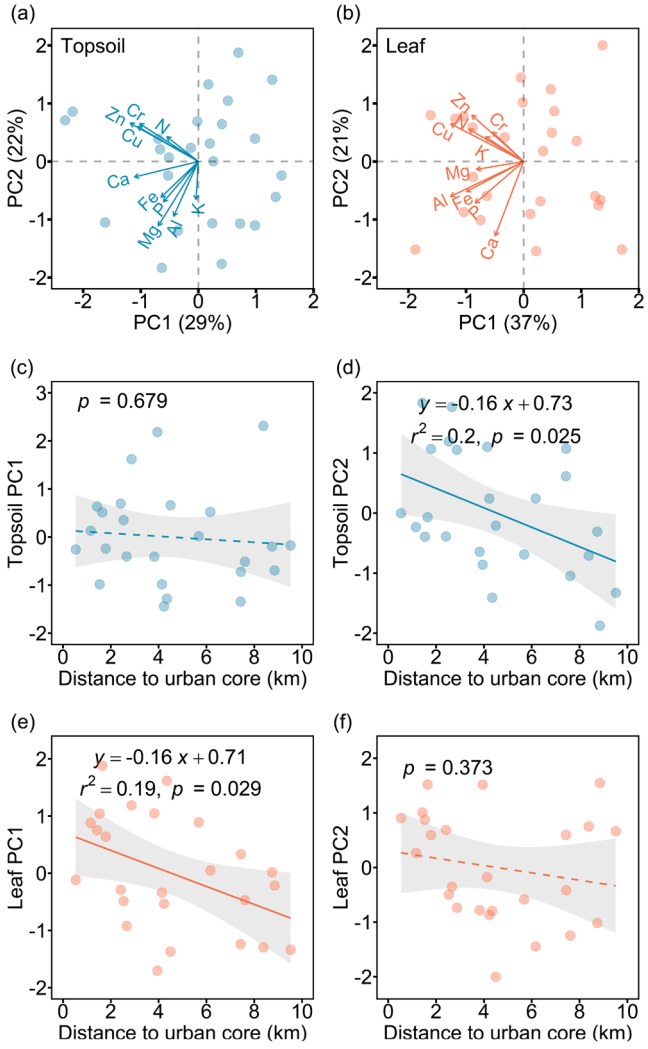

Fig. 5. Principal component analysis of topsoil and leaf elemental composition (a and b) and changes in PC1 and PC2 with the distance to urban core for topsoil elemental composition (c and d) and leaf elemental composition (e and f). The shaded areas indicate the 95 % confidence intervals of the curve fit.

accounting for 55 % of the total explained variance (Fig. 6b). Leaf PC1 of street trees was significantly higher along older roads (variance explained = 20 %, $p = 0.017$; Fig. 6d; Table S5) and in deciduous species (variance explained = 4 %, $p < 0.01$; Fig. S3; Table S5). Further analysis showed no significant correlation between leaf and topsoil content for each element, with the exception of P (Fig. S4). No significant correlations were found between elemental compositions of leaf and topsoil (leaf PC1 vs topsoil PC1: $p = 0.36$; leaf PC2 vs topsoil PC2: $p = 0.60$; leaf PC1 vs topsoil PC2: $p = 0.76$; leaf PC2 vs topsoil PC1: $p = 0.39$; Fig. 7), suggesting a decoupling of leaf and topsoil elemental compositions in street tree systems.

4. Discussion

4.1. Urban-rural gradients in tree pit topsoil elemental composition

Partially in line with our urban hotspot hypothesis, the contents of N, P, and Al in tree pit topsoil showed a significant increase towards the urban core. The higher topsoil contents of N and P in central urban areas are likely attributable to a hotspot effect of intensive anthropogenic inputs via traffic-sourced emission and deposition as well as other sources such as pet dogs, occasional fertilization and dumping of

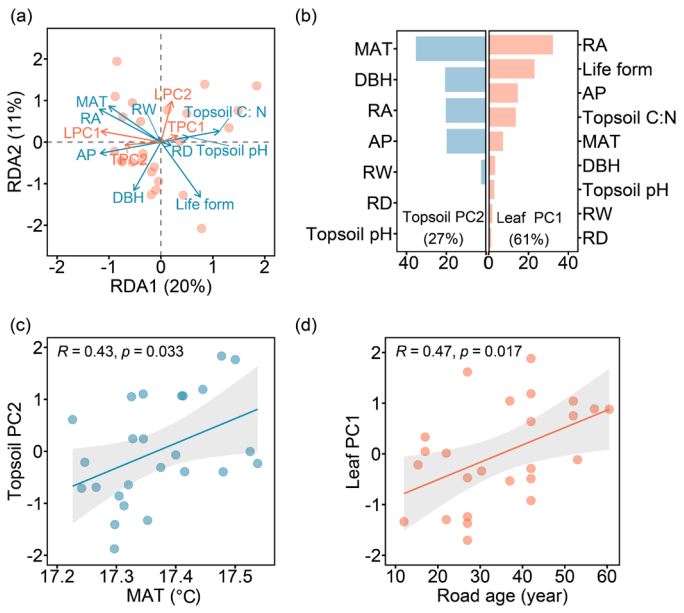

Fig. 6. Redundancy analysis plots showing the relationships between leaf and topsoil PC1 and PC2 and the potential drivers (a), hierarchical partitioning analysis plots showing the relative importance of the potential drivers in explaining the spatial variation of topsoil PC2 and leaf PC1(b), and the correlations between topsoil PC2 and leaf PC1 and the corresponding most important driver (c–d). The shaded areas indicate the 95 % confidence intervals of the curve fit. Abbreviations: RA, road age; RW, road width; RD, road density; DBH, diameter at breast height; MAT, mean annual temperature in the sampling year; AP, annual precipitation in the sampling year.

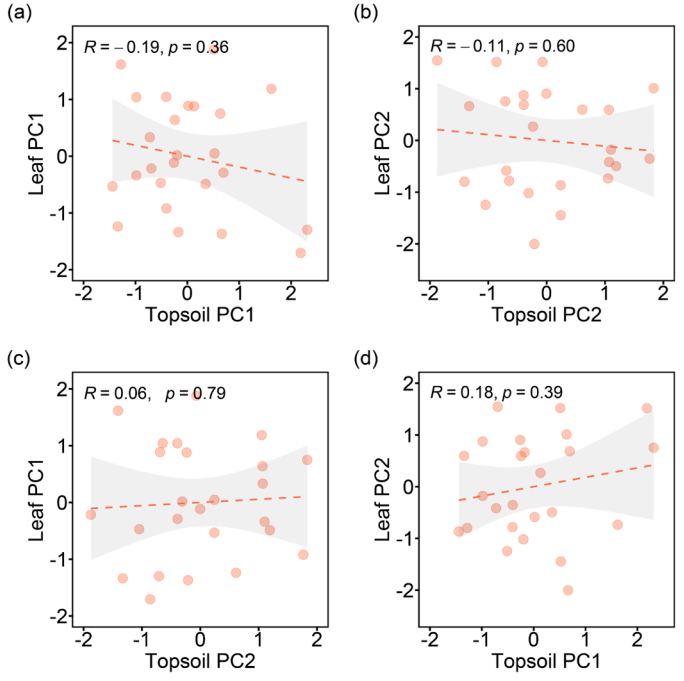

Fig. 7. Correlations (Pearson's correlation) between the principal components of elemental composition between leaf and topsoil of street trees.

scattered household waste (Nielsen., 2019; Fabianska et al., 2019; Xiong et al., 2020; Du et al., 2016, 2022a; Xia et al., 2022). Non-exhaust emissions (e.g., particles from brake pads, tires, belts, road paint, asphalt) are also important sources for Al (González et al., 2017; Jeong et al., 2022).). Overall, there is thus an accumulation of anthropogenic N, P, and Al inputs over time which shape significant urban-rural gradients. Anthropogenic N and P inputs to tree pit topsoil are important for street trees because they can partially compensate the nutrient loss caused by litter removal. However, the long-term accumulation of topsoil Al may have a negative effect on root nutrient uptake and transport, interfering with membrane-localized solute transporter (Lazof et al., 1994; Bojórquez-Quintal et al., 2017; Kar et al., 2021).

Unexpectedly, other nutrients (e.g., K, Ca, Mg, Zn, Fe, Cu, and Cr) showed no significant urban-rural gradients in tree pit topsoil likely attributable to relatively limited anthropogenic inputs. The strict standards for Fe, Cu, and Cr in gasoline or gasoline additives largely limited the input and accumulation of topsoil Fe, Cu, and Cr (Ministry of Ecology and Environment of the People's Republic of China, 2011). The inputs of K, Ca, Mg, and Zn into street tree pit topsoil are limited because they are mainly from some gasoline additive, and meanwhile, the small area of street tree pit further limits the amounts of potential inputs (Ministry of Ecology and Environment of the People's Republic of China, 2013). Moreover, some of these elements (e.g., K, Ca, Mg, and Zn) are easily leached from surface soils (Lucas et al., 2011; Tian and Niu, 2015) and this may partially violate the hypothesized urban-rural gradients.

Topsoil elemental composition in tree pits were featured by two principal components (Table S4) and the second principal component (PC2, mainly consist of P, K, Mg, Fe, and Al) increased significantly toward the urban core, being in line with the urban-rural gradients of topsoil P and Al (see discussion above). Our analysis further indicates that the seven potential drivers only explained a relatively low proportion (27 %) of the spatial variation in topsoil elemental composition, implying that other important drivers were not considered in our analysis due to a lack of corresponding data (Fig. 6b). For instance, soil elemental composition is strongly determined by parent material, the related physical and biochemical processes (e.g., mineralization of soil organic matter, mineral weathering, adsorption-desorption, and precipitation-dissolution reaction) and the conditions of soil development (Brady and Weil, 2019; Du et al., 2020; Sparks et al., 2024). Moreover, soil microorganisms play a vital role in element cycling and organic matter transformations, and thus information on soil microorganisms will further help us better uderstand the soil elemental cycles (Philippot et al., 2024). The accumulation of anthropogenic-sourced inputs (e.g., pet dogs, non-exhaust emissions, household waste and occasional fertilization) might theoretically shape an urban-rural gradient of corresponding topsoil element content over time, while in many cases (e.g., K, Ca, Mg, Zn, Fe, Cu, and Cr) such an effect is not significant because of relatively low inputs of traffic sourced elements due to the sealed impervious surface and large spatial heterogeneity of ambient topsoil conditions.

4.2. *Urban-rural gradients in street tree leaf elemental composition*

The contents of N, P, K, and Al in street tree leaves showed an increase from rural areas toward the central urban areas, partially supporting our urban hotspot hypothesis. Previous studies also found higher leaf N and P contents of trees growing in the urban areas in other large cities or regions, such as the Campania Region of Italy (Maisto et al., 2013), Guiyang of China (Xu et al., 2018), and Salt Lake Valley of USA (Cobley and Pataki, 2019). Our analysis indicates that leaf contents of N and Al increased with older road age, being a surrogate of the accumulation effect of element inputs from human activities (Baum et al., 2000; Liang et al., 2020; Du et al., 2022a). Similar to those in tree pit topsoil, the contents of Ca, Mg, Fe, Zn, Cu, and Cr in street tree leaves also showed no significant trend across the urban-rural gradients. This is likely attributable to low inputs of these elements which are not able to shape strong urban-rural trends in the street tree systems (Ministry of Ecology and Environment of the People's Republic of China, 2013; Coufalík et al., 2019).

Leaf elemental composition of street trees was reduced into two principal components with first principal component (PC1, mainly

dominated by N, K, Mg, Fe, Cu, and Al) exhibiting a significant linear increase toward the central urban area. Compared with rural areas, traffic emissions are more intensive in urban areas and thus are a stronger source of various elements for street tree systems. Street trees can either take up nutrients from tree pit soils via roots or assimilate vehicular-emitted elements via stomata on the leaf surface (Oliva and Espinosa, 2007; Fig. 1a), potentially shaping significant spatial patterns along urban-rural gradients. Moreover, pet dogs, occasional fertilization and household waste around street trees may also improve soil nutrient contents and tree leaf nutrition in urban areas (Przybysz et al., 2014; Nielsen, 2019; Xiong et al., 2020; Kaushal et al., 2020). Our analysis also shows that leaf PC1 increased significantly with road age (Fig. 6d), implying an accumulating effect of human activities on the leaf elemental composition over time.

4.3. Decoupling between elemental composition of street tree leaves and topsoil

In contrast to our plant-soil coupling hypothesis, elemental composition of street tree leaves and topsoil were not significantly correlated. In natural forests, nutrients are recycled by root uptake and litterfall return and thus shape strong coupled elemental composition between tree leaves and topsoil (Bradford et al., 2016; Chen et al., 2018). However, the recycling of nutrients is largely blocked in street tree systems due to the removal of litterfall and the impervious surface (Kaye et al., 2006; Lorenz and Lal, 2009; Nowak and Greenfield, 2012; Fig. 1a), weakening the linkages between elemental composition of street tree leaves and topsoil. Moreover, our results showed that the drivers in shaping the spatial patterns of leaf and topsoil elemental compositions were different. Specifically, leaf elemental composition was strongly influenced by the accumulating effect of human activities over time, but the topsoil elemental composition was minorly explained by road age. Meanwhile, previous studies indicated that soil elemental availability was not necessarily determined by total soil concentrations but by amounts of available nutrients in soluble forms (Sauve et al., 1996). The assimilated nutrients by street tree leaves only are a part of total elements in soil, thus not necessarily guaranteeing significant correlations between leaf and topsoil elemental compositions.

Our analysis of soil is limited to the surface layer (i.e., 0–10 cm), although street trees also take up nutrients from deeper soil layers. Deep soils below impervious pavements are, however, hardly altered by anthropogenic-sourced elements and management operations after their establishment. For instance, the transfer of anthropogenic-sourced elements from topsoil to deeper layers is commonly blocked in street tree systems due to litter removal and impervious pavements. Overall, our findings of urban-rural shifts in the topsoil and leaf elemental composition provide a baseline for nutrient management and pollutant assessment in the street tree systems.

5. Conclusion

By sampling the street tree leaves and topsoil across urban-rural gradients, we elucidated the spatial patterns of street tree leaf and topsoil elemental composition and their key drivers in a typical large city in the subtropical region of China. Our results demonstrate that leaf N, P, K, and Al as well as topsoil N, P, and Al contents exhibited an increase toward central urban area, being in line with an urban hotspot hypothesis. However, no significant spatial pattern was found for the contents of leaf Ca, Mg, Fe, Zn, Cu, and Cr as well as topsoil K, Ca, Mg, Fe, Zn, Cu, and Cr. Road age was identified as a key driver in shaping the spatial pattern of leaf elemental composition. It's worth noting that there was a significant accumulation of Al in both street tree leaves and topsoil over time, which may become a threat to street tree ecosystem health in the future. Moreover, there was a decoupling between leaf and topsoil elemental composition in the street tree system. In recent years, the standards of vehicular emissions in China have become increasingly stricter to guarantee better air quality, especially in large cities (Ministry of Ecology and Environment of the People's Republic of China, 2011). Further studies are needed to understand the long-term changes in spatial patterns of leaf and topsoil elemental compositions in street tree systems over time and how such changes correlate to the health and function of street trees.

CRediT authorship contribution statement

Tao He: Investigation, Methodology, Formal analysis, Data curation, Writing – original draft, Writing – review & editing. Enzai Du: Conceptualization, Methodology, Formal analysis, Validation, Supervision, Funding acquisition, Writing – original draft, Writing – review & editing. **Xueyi Yang:** Investigation, Writing – review & editing. **Yuying Guo:** Methodology, Writing – review & editing. **Nan Xia:** Methodology, Writing – review & editing. **Wim de Vries:** Writing – review & editing.

Declaration of Competing Interest

The authors declare that they have no known competing financial interests or personal relationships that could have appeared to influence the work reported in this paper.

Acknowledgment

This work was supported by National Natural Science Foundation of China (42373078), the Fundamental Research Funds for the Central Universities, and BNU-FGS Global Environmental Change Program (2023-GC-ZYTS-09).

Appendix A. Supporting information

Supplementary data associated with this article can be found in the online version at doi:10.1016/j.ufug.2025.128677.

Data availability

The data that support the findings of this study can be available from the corresponding author.

References

Anbarasan, S., Ramesh, S., 2021. The role of plant roots in nutrient uptake and soil health. Plant Sci. Arch. 6 (1), 5–08. https://doi.org/10.51470/PSA.2021.6.1.05.

Baum, M.M., Kiyomiya, E.S., Kumar, S., Lappas, A.M., 2000. Multicomponent remote sensing of vehicle exhaust by dispersive absorption spectroscopy. 1. Effect of fuel type and catalyst performance. Environ. Sci. Technol. 34 (13), 2851–2858. https://doi.org/10.1021/es991351k.

Bettez, N.D., Marino, R., Howarth, R.W., Davidson, E.A., 2013. Roads as nitrogen deposition hot spots. Biogeochemistry 114 (1–3), 149–163. https://doi.org/10.1007/s10533-013-9847-z.

Bojórquez-Quintal, E., Escalante-Magaña, C., Echevarría-Machado, I., Martínez-Estévez, M., 2017. Aluminum, a friend or foe of higher plants in acid soils. Front. Plant Sci. 8, 1767. https://doi.org/10.3389/fpls.2017.01767.

Bradford, M.A., Berg, B., Maynard, D.S., Wieder, W.R., Wood, S.A., 2016. Understanding the dominant controls on litter decomposition. J. Ecol. 104 (1), 229–238. https://doi.org/10.1111/1365-2745.12507.

Brady, N.C., Weil, R.R., 2019. The Nature and Properties of Soils. China Science Publishing & Media Ltd, pp. 33–77.

Cetin, M., Aljama, A.M.O., Alrabiti, O.B.M., Adiguzel, F., Sevik, H., Zeren Cetin, I., 2022. Using topsoil analysis to determine and map changes in Ni Co pollution. Water Air Soil Pollut. 233 (8), 293. https://doi.org/10.1007/s11270-022-05762-y.

Chen, X., Gong, L., Liu, Y.T., 2018. The ecological stoichiometry and interrelationship between litter and soil under seasonal snowfall in Tianshan Mountain. Ecosphere 9 (11), e02520. https://doi.org/10.1002/ecs2.2520.

Chengdu Municipal Bureau of Statistics, 2023. Chengdu Statistical Yearbook. China Statistics Press.

Cobley, L.A.E., Pataki, D.E., 2019. Vehicle emissions and fertilizer impact the leaf chemistry of urban trees in Salt Lake Valley, UT. Environ. Pollut. 254 (A), 112984. https://doi.org/10.1016/j.envpol.2019.112984.

Coufalík, P., Matousek, T., Krumal, K., Vojtísek-Lom, M., Beránek, V., Mikuska, P., 2019. Content of metals in emissions from gasoline, diesel, and alternative mixed biofuels.

Environ. Sci. Pollut. 26 (28), 29012–29019. https://doi.org/10.1007/s11356-019-06144-4.
Dan-Badjo, A.T., Rychen, G., Ducoulombier, C., 2008. Pollution maps of grass contamination by platinum group elements and polycyclic aromatic hydrocarbons from road traffic. Agron. Sustain. Dev. 28 (4), 457–464. https://doi.org/10.1051/agro:2008032.
Day, S.D., Wiseman, P.E., Dickinson, S.B., Harris, J.R., 2010. Tree root ecology in the urban environment and implications for a sustainable rhizosphere. Arboric. Urban For. 36 (5), 193–205. https://doi.org/10.48044/jauf.2010.026.
De Silva, S., Ball, A.S., Huynh, T., Reichman, S.M., 2016. Metal accumulation in roadside soil in Melbourne, Australia: effect of road age, traffic density and vehicular speed. Environ. Pollut. 208, 102–109. https://doi.org/10.1016/j.envpol.2015.09.032.
De Vries, W., Boumans, L.J.M., Olsthoorn en, A., Leeters, E.E.J.M., 1994. Chemical Composition of Needles, Soil, Soil Moisture and Groundwater from Twelve Monitoring Sites under Forest. The Initial State in 1992 (in Dutch). Rapport 370.1. DLO-Staring Centrum, Wageningen, p. 55.
Douvris, C., Vaughan, T., Bussan, D., Bartzas, G., Thomas, R., 2023. How ICP-OES changed the face of trace element analysis: review of the global application landscape. Sci. Total Environ. 905, 167242. https://doi.org/10.1016/j.scitotenv.2023.167242.
Du, E.Z., de Vries, W., McNulty, S., Fenn, M.E., 2018. Bulk deposition of base cationic nutrients in China's forests: annual rates and spatial characteristics. Atmos. Environ. 184, 121–128. https://doi.org/10.1016/j.atmosenv.2018.04.042.
Du, E.Z., de Vries, W., Han, W.X., Liu, X.J., Yan, Z.B., Jiang, Y., 2016. Imbalanced phosphorus and nitrogen deposition in China's forests. Atmos. Chem. Phys. 16 (13), 8571–8579. https://doi.org/10.5194/acp-16-8571-2016.
Du, E.Z., Xia, N., Guo, Y.Y., Tian, Y.H., Li, B.H., Liu, X.J., De Vries, W., 2022a. Ecological effects of nitrogen deposition on urban forests: an overview. Front. Agric. Sci. Eng. 9 (3), 445–456. https://doi.org/10.15302/J-FASE-2021429.
Du, E.Z., Xia, N., Tang, Y., Guo, Z.D., Guo, Y.Y., Wang, Y., de Vries, W., 2022b. Anthropogenic and climatic shaping of soil nitrogen properties across urban-rural-natural forests in the Beijing metropolitan region. Geoderma 406, 115524. https://doi.org/10.1016/j.geoderma.2021.115524.
Du, L., Zhang, X.Z., Zheng, Z.C., Li, T.X., Wang, Y.D., Huang, H.G., Yu, H.Y., Ye, D.H., Liu, T., 2020. Paddy soil nutrients and stoichiometric ratios as affected by anthropogenic activities during long-term tillage process in Chengdu Plain. J. Soil Sediment. 20 (11), 3835–3845. https://doi.org/10.1007/s11368-020-02724-x.
Dynarski, K.A., Soper, F.M., Reed, S.C., Wieder, W.R., Cleveland, C.C., 2023. Patterns and controls of foliar nutrient stoichiometry and flexibility across United States forests. Ecology 104 (2), 3909. https://doi.org/10.1002/ecy.3909.
Fabianska, M.J., Kozielska, B., Konieczynski, J., Bielaczyc, P., 2019. Occurrence of organic phosphates in particulate matter of the vehicle exhausts and outdoor environment A case study. Environ. Pollut. 244, 351–360. https://doi.org/10.1016/j.envpol.2018.10.060.
Fantozzi, F., Monaci, F., Blanusa, T., Bargagli, R., 2013. Holm Oak (*Quercus ilex* L.) canopy as interceptor of airborne trace elements and their accumulation in the litter and topsoil. Environ. Pollut. 183, 89–95. https://doi.org/10.1016/j.envpol.2012.11.037.
González, L.T., Rodríguez, F.E.L., Sánchez-Domínguez, M., Cavazos, A., Leyva-Porras, C., Silva-Vidaurri, L.G., Askar, K.A., Kharissov, B.I., Chiu, J.F.V., Barbosa, J.M.A., 2017. Determination of trace metals in TSP and PM2.5 materials collected in the Metropolitan Area of Monterrey, Mexico: a characterization study by XPS, ICP-AES and SEM-EDS. Atmos. Res. 196, 8–22. https://doi.org/10.1016/j.atmosres.2017.05.009.
Guo, H., He, T., Gao, X., Xia, N., Tang, Y., Tian, Y., Du, E., 2024. Distinct features of topsoil carbon fractions across urban forests in eastern China. Eur. J. Soil Sci. 75 (5), e13586. https://doi.org/10.1111/ejss.13586.
Indris, S.N., Rudolph, D.L., Glass, B.K., Van Cappellen, P., 2020. Evaluating phosphorous from vehicular emissions as a potential source of contamination to ground and surface water. Cogent Environ. Sci. 6 (1), 1794702. https://doi.org/10.1080/23311843.2020.1794702.
Janhäll, S., 2015. Review on urban vegetation and particle air pollution - deposition and dispersion. Atmos. Environ. 105, 130–137. https://doi.org/10.1016/j.atmosenv.2015.01.052.
Jeong, H., Ryu, J.S., Ra, K., 2022. Characteristics of potentially toxic elements and multi-isotope signatures (Cu, Zn, Pb) in non-exhaust traffic emission sources. Environ. Pollut. 299, 118339. https://doi.org/10.1016/j.envpol.2021.118339.
Jobbagy, E.G., Jackson, R.B., 2001. The distribution of soil nutrients with depth: global patterns and the imprint of plants. Biogeochemistry 53 (1), 51–77. https://doi.org/10.1023/a:1010760720215.
Kar, D., Pradhan, A.A., Datta, S., 2021. The role of solute transporters in aluminum toxicity and tolerance. Physiol. Plant. 171 (4), 638–652. https://doi.org/10.1111/ppl.13214.
Kaushal, S.S., McDowell, W.H., Wollheim, W.M., 2014. Tracking evolution of urban biogeochemical cycles: past, present, and future. Biogeochemistry 121 (1), 1–21. https://doi.org/10.1007/s10533-014-0014-y.
Kaushal, S.S., Wood, K.L., Galella, J.G., Gion, A.M., Haq, S., Goodling, P.J., Haviland, K.A., Reimer, J.E., Morel, C.J., Wessel, B., Nguyen, W., Hollingsworth, J.W., Mei, K., Leal, J., Widmer, J., Sharif, R., Mayer, P.M., Johnson, T.A.N., Newcomb, K.D., Smith, E., Belt, K.T., 2020. Making 'chemical cocktails' - evolution of urban geochemical processes across the periodic table of elements. Appl. Geochem. 119, 104632.
Kaye, J.P., Groffman, P.M., Grimm, N.B., Baker, L.A., Pouyat, R.V., 2006. A distinct urban biogeochemistry? Trends Ecol. Evol. 21 (4), 192–199. https://doi.org/10.1016/j.tree.2005.12.006.
Lai, J.S., Zou, Y., Zhang, J.L., Peres-Neto, P.R., 2022. Generalizing hierarchical and variation partitioning in multiple regression and canonical analyses using the rdacca.hp R package. Methods Ecol. Evol. 13 (4), 782–788. https://doi.org/10.1111/2041-210X.13800.
Lazof, D.B., Rincón, M., Rufty, T.W., Mackown, C.T., Carter, T.E., 1994. Aluminum accumulation and associated effects on $^{15}NO_3^-$influx in roots of two soybean genotypes differing in Al tolerance. Plant Soil 164 (2), 291–297. https://doi.org/10.1007/bf00010081.
Lilliefors, H.W., 1967. On the Kolmogorov-Smirnov test for normality with mean and variance unknown. J. Am. Stat. Assoc. 62, 399–402. https://doi.org/10.2307/2283970.
Liu, S.Y., Brandt, M., Nord-Larsen, T., Chave, J., Reiner, F., Lang, N.C., Tong, X.Y., Ciais, P., Igel, C., Pascual, A., Guerra-Hernandez, J., Li, S.Z., Mugabowindekwe, M., Saatchi, S., Yue, Y.M., Chen, Z.C., Fensholt, R., 2023. The overlooked contribution of trees outside forests to tree cover and woody biomass across Europe. Sci. Adv. 9 (37), eadh4097. https://doi.org/10.1126/sciadv.adh4097.
Liang, X.Y., Zhang, T., Lu, X.K., Ellsworth, D.S., BassiriRad, H., You, C.M., Wang, D., He, P.C., Deng, Q., Liu, H., Mo, J.M., Ye, Q., 2020. Global response patterns of plant photosynthesis to nitrogen addition: a meta-analysis. Glob. Change Biol. 26 (6), 3585–3600. https://doi.org/10.1111/gcb.15071.
Lorenz, K., Lal, R., 2009. Biogeochemical C and N cycles in urban soils. Environ. Int. 35 (1), 1–8. https://doi.org/10.1016/j.envint.2008.05.006.
Lucas, R.W., Klaminder, J., Futter, M.N., Bishop, K.H., Egnell, G., Laudon, H., Högberg, P., 2011. A meta-analysis of the effects of nitrogen additions on base cations: implications for plants, soils, and streams. For. Ecol. Manag. 262 (2), 95–104. https://doi.org/10.1016/j.foreco.2011.03.018.
Maisto, G., Baldantoni, D., Marco, A.D., Alfani, A., Virzo De Santo, A.V., 2013. Ranges of nutrient concentrations in Quercus ilex leaves at natural and urban sites. J. Soil Sci. Plant Nutr. 176 (5), 801–808. https://doi.org/10.1002/jpln.201200355.
McPherson, E.G., van Doorn, N., de Goede, J., 2016. Structure, function and value of street trees in California, USA. Urban For. Urban Green. 17, 104–115. https://doi.org/10.1016/j.ufug.2016.03.013.
Miller, A.L., Stipe, C.B., Habjan, M.C., Ahlstrand, G.G., 2007. Role of lubrication oil in particulate emissions from a hydrogen-powered internal combustion engine. Environ. Sci. Technol. 41 (19), 6828–6835. https://doi.org/10.1021/es070999r.
Ministry of Ecology and Environment of the People's Republic of China, 2013. Environmental Protection Technical Standard for Diesel Engines NOx Reduction Agent.
Ministry of Ecology and Environment of the People's Republic of China, 2011. Hazardous materials control standard for motor vehicle gasoline (IV, V). GWKB 1.1-2011.
Mullaney, J., Lucke, T., Trueman, S.J., 2015. A review of benefits and challenges in growing street trees in paved urban environments. Landsc. Urban Plan. 134, 157–166. https://doi.org/10.1016/j.landurbplan.2014.10.013.
Nickolas, S., 2021. How Stratified Random Sampling Works. Investopedia. ⟨https://www.investopedia.com/ask/answers/032615/what-are-some-examples-stratified-random-sampling.asp⟩.
Nielsen, 2019. 2019 Chinese Pet Products Consumption Trends Report. ⟨http://www.199it.com/archives/969439.html⟩.
Nowak, D.J., Greenfield, E.J., 2012. Tree and impervious cover change in US cities. Urban For. Urban Green. 11 (1), 21–30. https://doi.org/10.1016/j.ufug.2011.11.005.
Oliva, R.S., Espinosa, A.J.F., 2007. Monitoring of heavy metals in topsoils, atmospheric particles and plant leaves to identify possible contamination sources. Microchem. J. 86 (1), 131–139. https://doi.org/10.1016/j.microc.2007.01.003.
Olowoyo, J.O., van Heerden, E., Fischer, J.L., Baker, C., 2010. Trace metals in soil and leaves of Jacaranda mimosifolia in Tshwane area, South Africa. Atmos. Environ. 44 (14), 1826–1830. https://doi.org/10.1016/j.atmosenv.2010.01.048.
Philippot, L., Chenu, C., Kappler, A., Rillig, M.C., Fierer, N., 2024. The interplay between microbial communities and soil properties. Nat. Rev. Microbiol. 22, 226–239. https://doi.org/10.1038/s41579-023-00980-5.
Przybysz, A., Saebo, A., Hanslin, H.M., Gawronski, S.W., 2014. Accumulation of particulate matter and trace elements on vegetation as affected by pollution level, rainfall and the passage of time. Sci. Total Environ. 481, 360–369. https://doi.org/10.1016/j.scitotenv.2014.02.072.
Rai, P.K., 2016. Impacts of particulate matter pollution on plants: implications for environmental biomonitoring. Ecotoxicol. Environ. Saf. 129, 120–136. https://doi.org/10.1016/j.ecoenv.2016.03.012.
Sanchez-Lopez, A.S., Carrillo-Gonzalez, R., Gonzalez-Chavez, M.D.A., Rosas-Saito, G.H., Vangronsveld, J., 2015. Phytobarriers: plants capture particles containing potentially toxic elements originating from mine tailings in semiarid regions. Environ. Pollut. 205, 33–42. https://doi.org/10.1016/j.envpol.2015.05.010.
Sauve, S., Cook, N., Hendershot, W.H., McBride, M.B., 1996. Linking plant tissue concentrations and soil copper pools in urban contaminated soils. Environ. Pollut. 94 (2), 153–157. https://doi.org/10.1016/S0269-7491(96)00081-4.
Serbula, S.M., Miljkovic, D.D., Kovacevic, R.M., Ilic, A.A., 2012. Assessment of airborne heavy metal pollution using plant parts and topsoil. Ecotoxicol. Environ. Saf. 76, 209–214. https://doi.org/10.1016/j.ecoenv.2011.10.009.
Shurpali, N.J., 2023. Urbanization associated changes in biogeochemical cycles. Glob. Change Biol. 29 (12), 3237–3239. https://doi.org/10.1111/gcb.16698.
Soil Survey Staff, 2014. Section 4.3 Soil pH in Soil Survey Field and Laboratory Methods Manual. Soil Survey Investigations Report No. 51, Version 2.0. R. Burt and Soil Survey Staff (ed.). U.S. Department of Agriculture, Natural Resources Conservation Service.
Song, Y.S., Maher, B.A., Li, F., Wang, X.K., Sun, X., Zhang, H.X., 2015. Particulate matter deposited on leaf of five evergreen species in Beijing, China: source identification

and size distribution. Atmos. Environ. 105, 53–60. https://doi.org/10.1016/j.atmosenv.2015.01.032.
Sparks, D.L., Singh, B., Siebecker, M.G., 2024. Chapter 1 - An introduction to environmental soil chemistry. Environmental Soil Chemistry (third edition), pp. 1–38.
Tang, Y.J., Chen, A.P., Zhao, S.Q., 2016. Carbon storage and sequestration of urban street trees in Beijing, China. Front. Ecol. Evol. 4, 00053. https://doi.org/10.3389/fevo.2016.00053.
Tian, D., Niu, S., 2015. A global analysis of soil acidification caused by nitrogen addition. Environ. Res. Lett. 10 (2), 024019. https://doi.org/10.1088/1748-9326/10/2/024019.
Trombulak, S.C., Frissell, C.A., 2000. Review of ecological effects of roads on terrestrial and aquatic communities. Conserv. Biol. 14 (1), 18–30. https://doi.org/10.1046/j.1523-1739.2000.99084.x.
Venables, W.N., Ripley, B.D., 2002. Modern Applied Statistics with S. Springer-Verlag.
Wang, C., Xu, L., Song, C.S., 2017a. Study on determination of harmful metal elements in gasoline by ICP-AES. Chem. Eng. 5, 30–33. https://doi.org/10.16247/j.cnki.23-1171/tq.20170530.
Wang, Y.F., Huang, K.L., Li, C.T., Mi, H.H., Luo, J.H., Tsai, P.J., 2003. Emissions of fuel metals content from a diesel vehicle engine. Atmospheric Environ 37 (33), 4637–4643. https://doi.org/10.1016/j.atmosenv.2003.07.007.
Wang, Q., Li, Y., Wang, L., Xiang, M., Yuan, D., Shao, S., Gou, Q., 2017b. Stoichiometric characteristic of soil C, N, and P of green space along urban-suburb-rural gradient in eastern Chengdu. Soils 49 (2), 358–363. https://doi.org/10.13758/j.cnki.tr.2017.02.022.
Wild, R.J., Dubé, W.P., Aikin, K.C., Eilerman, S.J., Neuman, J.A., Peischl, J., Ryerson, T. B., Brown, S.S., 2017. On-road measurements of vehicle NO_2/NOx emission ratios in Denver, Colorado, USA. Atmos. Environ. 148, 182–189. https://doi.org/10.1016/j.atmosenv.2016.10.039.
Willis, K.J., Petrokofsky, G., 2017. The natural capital of city trees. Science 356, 374–376. https://doi.org/10.1126/science.aam9724.
Xia, N., Du, E.Z., Guo, Y.Y., Tang, Y., Wang, Y., de Vries, W., 2022. Urban soil phosphorus hotspot and its imprint on tree leaf phosphorus concentrations in the Beijing region. Plant Soil 477 (1-2), 425–437. https://doi.org/10.1007/s11104-022-05421-5.
Xia, N., Du, E., Tang, Y., Guo, H., 2023. A distinctive latitudinal trend of nitrogen isotope signature across urban forests in eastern China. Glob. Chang. Biol. 29 (19), 5666–5676. https://doi.org/10.1111/gcb.16899.
Xiong, C.H., Guo, Z., Chen, S.S., Gao, Q., Kishe, M.A., Shen, Q.S., 2020. Understanding the pathway of phosphorus metabolism in urban household consumption system: a case study of Dar es Salaam, Tanzania. J. Clean. Prod. 274, 122874. https://doi.org/10.1016/j.jclepro.2020.122874.
Xu, Y., Xiao, H.Y., Guan, H., Long, C.J., 2018. Monitoring atmospheric nitrogen pollution in Guiyang (SW China) by contrasting use of Cinnamomum camphora leaves, branch bark and bark as biomonitors. Environ. Pollut. 233, 1037–1048. https://doi.org/10.1016/j.envpol.2017.10.005.
Yang, J., Huang, X., 2023. The 30 m annual land cover datasets and its dynamics in China from 1985 to 2022 [Data set]. Earth Syst. Sci. Data 13 (1), 3907–3925. https://doi.org/10.5281/zenodo.8176941.
Zong, H., Yao, M.Q., Tang, Y.Q., Chen, H., 2020. Assessing the composition, diversity, and allergenic risk of street trees in Qingyang District of Chengdu City. Urban For. Urban Green. 54, 126747. https://doi.org/10.1016/j.ufug.2020.126747.
Zuur, A.F., Ieno, E.N., Elphick, C.S., 2010. A protocol for data exploration to avoid common statistical problems. Methods Ecol. Evol. 1 (1), 3–14. https://doi.org/10.1111/j.2041-210X.2009.00001.x.